PLOS ONE

RESEARCH ARTICLE

Improving the accuracy of fatty liver index to reflect liver fat content with predictive regression modelling

Hykoush A. Asaturyan, Nicolas Basty, Marjola Thanaj, Brandon Whitcher, E. Louise Thomas, Jimmy D. Bell*

Research Centre for Optimal Health, University of Westminster, London, United Kingdom

* J.Bell@westminster.ac.uk

Citation: Asaturyan HA, Basty N, Thanaj M, Whitcher B, Thomas EL, Bell JD (2022) Improving the accuracy of fatty liver index to reflect liver fat content with predictive regression modelling. PLoS ONE 17(9): e0273171. https://doi.org/10.1371/journal.pone.0273171

Editor: Ferdinando Carlo Sasso, University of Campania Luigi Vanvitelli: Universita degli Studi della Campania Luigi Vanvitelli, ITALY

Received: June 3, 2022

Accepted: August 3, 2022

Published: September 13, 2022

Data Availability Statement: The relevant data are available from Github at https://github.com/pbf-testing/flip. There are restrictions prohibiting the provision of the full data. Researchers may apply to use the UK Biobank data resource by submitting a health-related research proposal that is in the public interest. More information may be found on the UK Biobank researchers and resource catalogue pages (https://www.ukbiobank.ac.uk).

Abstract

Background

The fatty liver index (FLI) is frequently used as a non-invasive clinical marker for research, prognostic and diagnostic purposes. It is also used to stratify individuals with hepatic steatosis such as non-alcoholic fatty liver disease (NAFLD), and to detect the presence of type 2 diabetes or cardiovascular disease. The FLI is calculated using a combination of anthropometric and blood biochemical variables; however, it reportedly excludes 8.5-16.7% of individuals with NAFLD. Moreover, the FLI cannot quantitatively predict liver fat, which might otherwise render an improved diagnosis and assessment of fatty liver, particularly in longitudinal studies. We propose FLI+ using predictive regression modelling, an improved index reflecting liver fat content that integrates 12 routinely-measured variables, including the original FLI.

Methods and findings

We evaluated FLI+ on a dataset from the UK Biobank containing 28,796 individual estimates of proton density fat fraction derived from magnetic resonance imaging across normal to severe levels and interpolated to align with the original FLI range. The results obtained for FLI+ outperform the original FLI by delivering a lower mean absolute error by approximately 47%, a lower standard deviation by approximately 20%, and an increased adjusted R^2 statistic by approximately 49%, reflecting a more accurate representation of liver fat content.

Conclusions

Our proposed model predicting FLI+ has the potential to improve diagnosis and provide a more accurate stratification than FLI between absent, mild, moderate and severe levels of hepatic steatosis.

Funding: The authors received no specific funding for this work.

Competing interests: The authors have declared that no competing interests exist.

Introduction

There is a significant rise in the incidence of patients diagnosed with fatty liver, otherwise known as hepatic steatosis, defined as a fat content greater than than 5% of liver weight [1]. Steatosis is characteristic of both alcoholic liver disease (ALD), associated with a high risk of developing alcohol-related hepatitis [2], and non-alcoholic fatty liver disease (NAFLD) [3], associated with the risk of long-term extrahepatic cardiometabolic diseases including heart attack, stroke, type 2 diabetes (T2D) and insulin resistance [4, 5].

The pathophysiological characteristics underlying NAFLD are clinical features of metabolic syndrome and are associated with insulin resistance, which exacerbates NAFLD by increasing hepatic lipogenesis and inhibiting adipose tissue lipolysis [6–8]. NAFLD is prevalent in 25% to 40% of the general population globally [9, 10], rising to a prevalence of 80% to 90% in severely obese populations [11, 12]; as such fatty liver disease is becoming an increasing global public health concern [13, 14]. Multiple studies have demonstrated a strong association between NAFLD and T2D [15, 16], in addition to hyperlipidemia [17], hypertension [18], and an increased risk of developing cardiovascular disease [19, 20] and chronic kidney disease [21, 22].

NAFLD is a progressive condition with its first stage often described as simple steatosis. This leads to inflammation in some individuals, followed by non-alcoholic steatohepatitis (NASH), hepatocyte ballooning, tissue scarring, including fibrosis and cirrhosis, and potentially hepatocellular carcinoma and mortality [5]. The ability to diagnose and characterise hepatic steatosis early helps to stratify patients according to their level of liver fat, assist in decision-making for diagnostic procedures and appropriately target interventions. There have been increased efforts in achieving cost-effective and straightforward diagnostic methods that would be useful for screening, follow-up and evaluating treatment response in clinical practice and research. For example, a FibroScan is a non-invasive device that measures liver "stiffness" using specialised ultrasound technology, which can assess hepatic steatosis and fibrosis [23].

The most commonly applied non-invasive methods used for diagnosing hepatic steatosis include the fatty liver index (FLI) [24], which combines anthropometry with serum a blood test; ultrasound, which is routinely used clinically for grading liver fat accumulation; and more recently, magnetic resonance imaging (MRI) and spectroscopy (MRS). MRI is generally regarded as the gold-standard for the quantitative measurement of liver fat (generally expressed as proton density fat fraction or PDFF). And though MRS is very accurate, it is generally restricted to smaller research studies in specialist centres [25, 26]. While the FLI is best described as a computed score or "predictive probability" for hepatic steatosis, a method such as MRI is required [27–30] to obtain a true quantitative measure of liver fat content and is routinely used in large cohort studies, pharmaceutical and clinical trials [31–33].

For nearly two decades, the clinical and research community have employed the FLI as a surrogate marker for the presence or absence of fatty liver [34–38]. The original FLI algorithm was derived from a study of 216 subjects with NAFLD and 280 controls, with fatty liver diagnosed using abdominal ultrasound. The FLI is calculated using waist circumference, body mass index (BMI), as well as triglycerides and gamma glutamyltransferase (GGT). The FLI has also been used to stratify prediabetes [39], T2D [37], metabolic syndrome [40] and cardiometabolic disease [41, 42].

However, a number of studies have highlighted distinct challenges and drawbacks when employing the FLI to detect the presence of fatty liver in certain subsets of subjects. For example, in a study of 338 volunteers, approximately 8.5% with fatty liver on ultrasound had a normal FLI score, whereas 27.8% of subjects with normal livers, had a FLI suggestive of excess liver fat [43]. Moreover, a recent meta-analysis of 10 different studies [38] comprising of

27,221 subjects showed that the livers of 16.7% of patients were classified as normal despite having confirmed NAFLD, whereas the FLI suggested that 33.3% of patients with normal livers had NAFLD. Furthermore, Cuthbertson *et al.* [44] reported that the FLI could not quantitatively predict liver fat when evaluated against proton MRS (^{1}H-MRS) from 336 subjects, 50% of whom had NAFLD.

In recent years, the increasing availability of large MRI datasets from national biobanks has enabled in-depth research towards understanding the impact of diet, lifestyle and genetics on the accumulation and distribution of liver fat [31]. Advancements in artificial intelligence applied to biomedical research have driven the development of regression models that predict body fat using multivariate supervised machine learning methods, such as support vector regression, gradient boosting regression and random forests, all of which are dependent on large datasets (involving more than 100 subjects) [45–50].

In this paper, we propose a regression tool for predicting FLI+, an improved version of the FLI that provides a more accurate reflection of liver fat content. Consequently, FLI+ may be used in clinical practice and research to reduce the number of cases where subjects with fatty liver are assessed as having normal livers and vice-versa, improving the overall stratification between absent, mild, moderate and severe fatty liver.

Materials and methods

Data collection of subjects

A dataset involving 28,796 subjects from the UK Biobank imaging cohort was employed (application number 23889). All subjects provided written informed consent, under the UKBB ethical approval from the North West Multi-Centre Research Ethics Committee (MREC). Over 98% of all subjects were of white European ancestry. The age range for inclusion was 44–82 years with varying levels of health status, including subjects who were healthy (≈40%), overweight (≈40%) and obese (≈20%). Additionally, this dataset included 4,913 (≈20%) subjects with at least one feature of metabolic syndrome following the International Diabetes Federation criteria [51]; for example, a waist circumference greater than 94 cm (males) or 80 cm (females), and a combination of T2D and hypertension.

Proton density fat fraction. All subjects underwent MRI scanning in a non-fasting state between August 2014 and December 2019 at a UK Biobank imaging centre using a Siemens 1.5T MAGNETOM Aera. A multi-echo spoiled-gradient-echo acquisition was used for the first 10,000 subjects and a single-slice IDEAL sequence was used in the remaining number of subjects [52]. Total acquisition time was less than three minutes with each individual acquisition taking place within a single expiratory breath-hold. No contrast agent was used. The proton density fat fraction (PDFF), expressed as a percentage of liver weight that is fat, was estimated using the PRESCO (Phase Regularized Estimation using Smoothing and Constrained Optimization) algorithm [53] with software available at https://github.com/recoh/pipeline [54].

Anthropometric and serum biochemical variables. Anthropometric measurements including weight, height, waist and hip circumferences were taken at the UK Biobank centres. Waist circumference was measured midway between the lower rib margin and the iliac crest, and hip circumference was measured at the greatest protrusion or largest circumference around the buttocks. From the extensive range of blood tests available in the UK Biobank, we selected a range of variables that have shown to be associated with fatty liver, including: gamma glutamyltransferase (GGT), triglycerides, glucose and glycosylated haemoglobin A1c (HbA1c) [55, 56]; white blood cell count [57, 58], uric acid [59, 60], high-density lipoprotein (HDL) [61] and testosterone [62–64]; aspartate aminotransferase (AST), alanine

aminotransferase (ALT), and also derived the ratio of AST to ALT [56, 65] and the ratio of AST to platelet count [66, 67]. Diagnoses of liver disease and T2D were obtained from UK Biobank health related outcome data collated from hospital admission records and self-reported sources [68]. The codes are also defined in Text A in S1 File and Table A in S1 File.

Fatty liver index calculation

The fatty liver index (FLI), as a score between 0 and 100, is defined using BMI (kg/m^2), serum triglycerides (mg/dL), GGT (U/L) and waist circumference (cm) [24]

$$FLI = \frac{\exp(\lambda)}{1 + \exp(\lambda)} \times 100, \tag{1}$$

where

$$\begin{aligned} \lambda &= 0.953 \times \ln(\text{triglycerides}) + 0.139 \times \text{BMI} + 0.718 \\ &\times \ln(\text{GGT}) + 0.053 \times (\text{waist circumference}) - 15.745. \end{aligned} \tag{2}$$

Comparing FLI with PDFF

Previous studies have established reference values for both PDFF and FLI that correspond to a normal liver and values relating to elevated or severe liver fat infiltration [27–30, 34–38]. However, a comparison between a quantitative measure such as PDFF and the FLI score, which have entirely different ranges, is not necessarily straightforward. To overcome this challenge and improve the comparison, we performed a linear interpolation for each risk group, mapping the PDFF values for each range to the corresponding FLI range, which is denoted as the Mapped (*M*)-PDFF throughout this paper (Table 1). Additional details are provided in Text B in S1 File.

Constructing FLI+ models

We aimed to develop a model for predicting FLI+ in which the ideal target output is *M*-PDFF. To reduce the skewness in the data, it was necessary to apply a log transform to the *M*-PDFF. Consequently, the predicted FLI+ values were exponentially transformed to obtain a score between 0 and 100.

To develop the proposed model, it was essential to select input variables strongly associated with fatty liver. Three different models were developed using "gradient boosting regression" by considering the input variable type and ease of accessibility, with each subsequent model having a reduced number of variables.

Gradient boosting regression model. The gradient boosting algorithm [69] is well-known in machine learning, in which the algorithm uses an ensemble of decision trees to

Table 1. MRI derived PDFF risk range mapped to equivalent FLI risk range.

Risk	PDFF	FLI	Mapped PDFF to FLI
Normal	0% ≤ PDFF ≤ 5%	0 ≤ FLI < 30	0 ≤ M-PDFF < 30
Elevated	5% < PDFF ≤ 10%	30 ≤ FLI < 60	30 ≤ M-PDFF < 60
Severe	10% < PDFF ≤ 45%	60 ≤ FLI ≤ 100	60 ≤ M-PDFF ≤ 100

The risk range from PDFF quantifying liver fat compared to the commonly used equivalent risk range for FLI. Mapped (*M*)-PDFF describes the interpolated predictive target range to develop and evaluate FLI+.

https://doi.org/10.1371/journal.pone.0273171.t001

minimise the error between a predicted outcome and the expected outcome. A gradient boosting regressor may be used to predict continuous target variables, as in the case of this study.

Experimental setup. The proposed method and subsequent analysis was developed using Python 3.7 via Windows 10 running on a GeForce GTX 1060 GPU and i7–8750H CPU at 2.20GHz. The source code is available at https://github.com/pbf-testing/flip. The full dataset was split into training and testing datasets comprising 21,597 (75%) and 7,199 (25%) subjects, respectively. The training and testing datasets share an equal ratio of normal (≈70%), elevated (≈17%) and severe (≈13%) cases of liver fat. The gradient boosting regressor utilised an initial learning rate (0.1) and a loss function of mean squared error (MSE) to minimise the error in every iteration until reaching a pre-specified maximum (100).

Statistical analysis

All anthropometric characteristics and biochemical variables were initially correlated with PDFF using Pearson's correlation coefficient. Group comparisons were performed using the Kruskal-Wallis test for categorical variables and a one-way ANOVA for continuous variables. Baseline subject characteristics were reported as median and interquartile range (IQR) for continuous variables, and frequency and percentage for categorical variables. Linear regression with 95% prediction intervals was used to assess the relationship between FLI and PDFF, where the prediction intervals reflect the range of FLI values assigned to a subject for an acquired PDFF.

Evaluating FLI+. We aimed to achieve a balance between utilising variables that influence fatty liver while minimising the number of variables that might otherwise have a low impact on accurately predicting FLI+. The percentage of importance in which each of the three gradient boosting regressors selected a variable was analysed. The resultant model predicting FLI + was evaluated using four-fold cross-validation (CV) to assess performance. That is, the entire dataset was divided into four equal folds, three of which were used for training and the remainder for testing. This process was repeated four different times, after which average measures of error were computed.

To compare FLI+ and the corresponding FLI with the target *M*-PDFF, the mean absolute error (MAE), standard deviation and adjusted coefficient of determination (R^2) were calculated. To analyse the ability of FLI+ to discriminate between subjects with and without fatty liver at different risk levels, receiver operator characteristic (ROC) curves were constructed with 95% confidence intervals (CIs). The following diagnostic statistics were computed for a range of five-unit intervals: sensitivity (SN), specificity (SP), positive likelihood ratio (LR+) and negative likelihood ratio (LR−).

Results

Clinical characteristics of subjects

Subjects were stratified into three groups using liver PDFF cut-off points as previously reported [70]. Participants with PDFF in the normal range were assigned to the normal group, and the remainder were stratified into the elevated or severe groups (see Table 1). The clinical, biochemical variables, anthropometric variables and characteristics of participants are shown in Table 2. Additional information about these variables, and their corresponding relationship with the target PDFF, are provided in Table B in S1 File. The three groups had a comparable median age, but the gender distribution in both the elevated and severe groups was unequal with a higher proportion of male subjects (69.6% and 68.8% respectively). Approximately 29.4% of all 28,796 subjects ($N = 8,453$) had fatty liver with 5,854 of those being male (69.3%).

Table 2. Comparison of anthropometric, biochemical and clinical subject characteristics.

	Normal	Elevated	Severe	*p*-value
N	20343	4967	3486	-
Male	10710 (52.6%)	3455 (69.6%)	2399 (68.8%)	< 0.0001
Female	9633 (47.4%)	1512 (30.4%)	1087 (31.2%)	< 0.0001
Age (years)	65 (58, 71)	66 (60, 71)	64 (58, 70)	< 0.0001
Weight (kg)	72.9 (64.1, 82.0)	84.1 (76.0, 93.9)	90.1 (80.6, 100.3)	< 0.0001
BMI (kg/m^2)	25.1 (23.1, 27.5)	28.4 (26.1, 31.0)	30.4 (27.9, 33.6)	< 0.0001
Waist (cm)	86 (78, 94)	96 (90, 103)	101 (94, 109)	< 0.0001
Hip (cm)	99 (94, 104)	103 (99, 108)	106 (101, 112)	< 0.0001
TG (mg/dL)	23.3 (16.9, 33.0)	32.8 (23.4, 45.4)	36.0 (25.7, 51.5)	< 0.0001
Uric acid (mg/dL)	3.3 (2.8, 3.9)	3.9 (3.3, 4.4)	4.0 (3.4, 4.6)	< 0.0001
Glucose (mg/dL)	87.5 (81.8, 93.5)	89.1 (83.0, 96.2)	90.0 (83.1, 98.5)	< 0.0001
HbA1c (mg/dL)	621.0 (579.6, 662.4)	637.2 (590.4, 682.2)	649.8 (601.2, 707.4)	< 0.0001
HDL (mg/dL)	26.0 (22.0, 31.0)	22.8 (19.5, 27.1)	21.7 (18.6, 25.3)	< 0.0001
TTST (nmol/L)	7.3 (1.0, 12.4)	9.1 (1.5, 12.1)	8.8 (1.6, 11.9)	< 0.0001
GGT (U/L)	23.3 (17.1, 34.6)	32.8 (23.6, 48.0)	37.4 (26.0, 56.8)	< 0.0001
AST (U/L)	23.9 (20.7, 27.9)	25.6 (22.1, 30.4)	27.4 (23.0, 33.6)	< 0.0001
ALT (U/L)	18.9 (14.7, 24.8)	24.3 (19.2, 32.5)	29.4 (21.5, 40.8)	< 0.0001
PLT ($10^9/L$)	243.6 (210.6, 280.9)	243.4 (209, 280)	244.5 (211.0, 282.0)	0.5917
WBC ($10^9/L$)	6.3 (5.3, 7.4)	6.7 (5.7, 7.7)	6.9 (5.9, 8.1)	< 0.0001
AST:ALT	1.27 (1.04, 1.52)	1.04 (0.86, 1.25)	0.93 (0.77, 1.15)	< 0.0001
AST:PLT	0.10 (0.08, 0.12)	0.11 (0.09, 0.14)	0.11 (0.09, 0.15)	< 0.0001
Waist:Hip	0.87 (0.80, 0.93)	0.93 (0.88, 0.98)	0.95 (0.90, 1.00)	< 0.0001
Type 2 diabetes	889 (4.4%)	584 (11.8%)	699 (20.1%)	< 0.0001
Liver disease	224 (1.1%)	90 (1.8%)	106 (3.0%)	< 0.0001
FLI	8.9 (3.5, 21.5)	32.2 (16.1, 54.5)	49.0 (28.6, 72.6)	< 0.0001
PDFF (%)	2.6 (2.1, 3.4)	6.7 (5.7, 8.0)	14.6 (11.9, 19.2)	< 0.0001

Categorical variables compared using the Kruskal-Wallis test and continuous variables compared using one-way ANOVA. Values are presented as median (interquartile range) for continuous variables and frequency (%) for categorical variables. **Abbreviations**: TG = triglycerides; HDL = high-density lipoprotein cholesterol; HbA1c = glycosylated haemoglobin A1c; TTST = testosterone; GGT = gamma glutamyltransferase; AST = aspartate aminotransferase; ALT = alanine aminotransferase; PLT = platelet count; WBC = white blood cell count; FLI = fatty liver index; PDFF = proton density fat fraction.

https://doi.org/10.1371/journal.pone.0273171.t002

Moreover, 70.6% ($N = 20, 343$) of all subjects were in the normal group, in which 10,710 were male (52.6%).

Subjects with fatty liver were primarily overweight or obese, with significantly higher BMI and waist-to-hip ratio compared to subjects with normal levels of PDFF. They exhibited statistically higher ($p < 0.0001$) serum uric acid with a median of 3.9 mg/dL (IQR 3.3–4.5 mg/dL) versus 3.3 mg/dL (IQR 2.8–3.9 mg/dL), glucose with a median of 89.4 mg/dL (IQR 83.0–97.1 mg/dL) versus 87.5 mg/dL (IQR 81.8–93.5 mg/dL), GGT with a median of 34.6 U/L (IQR 24.4–51.6 U/L) versus 23.3 U/L (IQR 17.1–34.6 U/L) and triglycerides with a median of 34.0 mg/dL (IQR 24.4–48.4 mg/dL) versus 23.3 mg/dL (IQR 16.9–33.0 mg/dL). All three groups had a comparable rate of T2D, but the liver disease diagnosis was approximately two and five times higher in the elevated and severe group compared to the normal group, respectively.

Given how the groups were constructed, the PDFF (%) was significantly lower ($p < 0.0001$) in the normal group (median 2.6%, IQR 2.1–3.4%) compared to the elevated (median 6.7%, IQR 5.7–8.0%) and severe (median 14.6%, IQR 11.9–19.2%) groups. Fig 1(a) displays a distribution of PDFF across all subjects and Fig 1(b) indicates the amount of variation in PDFF for

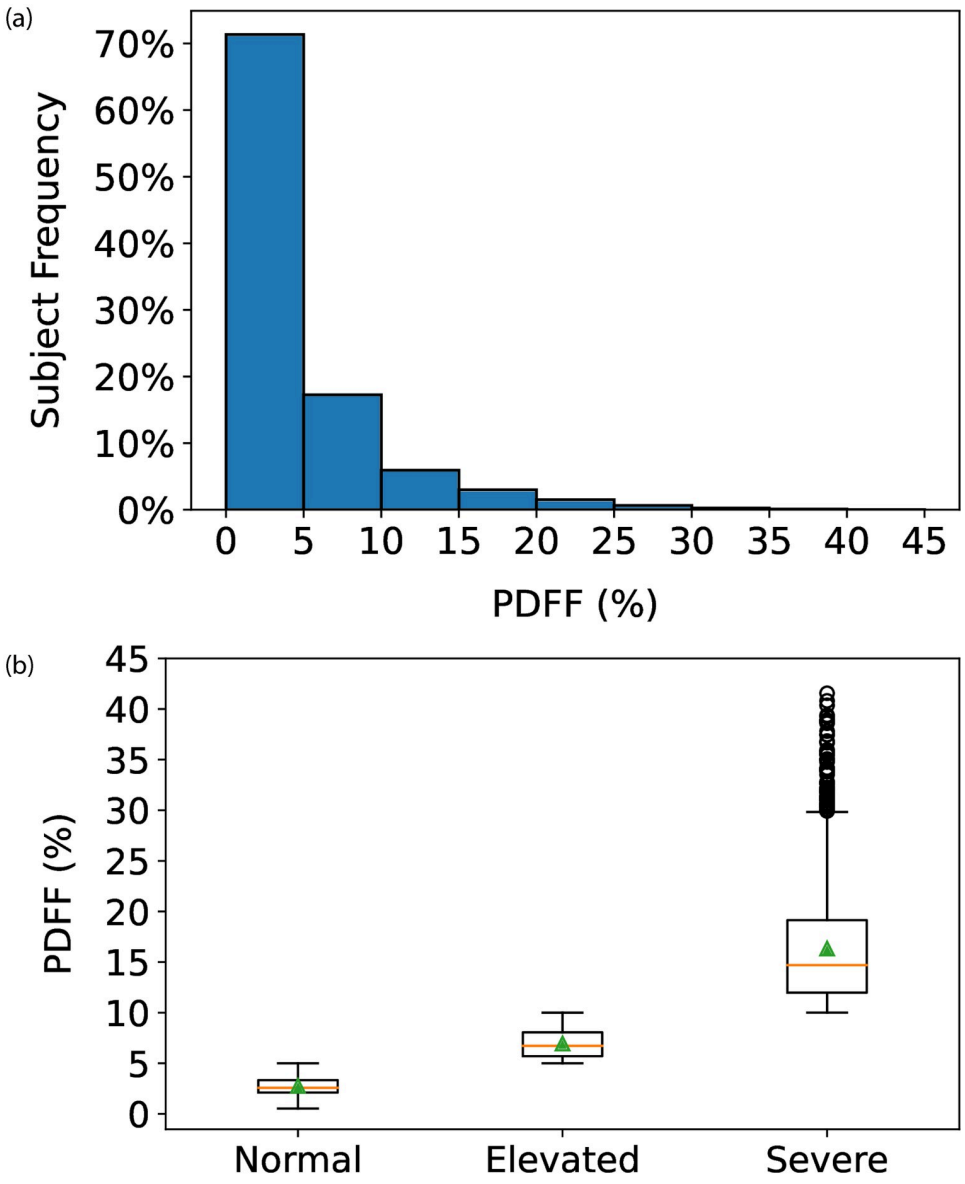

Fig 1. Proton density fat fraction (PDFF) in (a) all subjects and (b) three groups.

https://doi.org/10.1371/journal.pone.0273171.g001

each of the three groups provided in Table 2. Differences in PDFF were reflected in the serum biochemical results with significantly higher AST, ALT, GGT and triglycerides, and lower HDL cholesterol in the elevated and severe groups. Subjects within a normal PDFF range had significantly lower FLI with a median of 8.9 (IQR 3.5–21.5) compared to 32.2 (IQR 16.1–54.5) and 49.0 (IQR 28.6–72.6) in the elevated and severe groups, respectively.

Correlating FLI with PDFF

The relationship between the FLI and corresponding PDFF for all subjects is shown in Fig 2(a) ($R^2 = 0.279$). Taking into account the interpolated PDFF values for each range to the corresponding FLI range for a particular risk group, the variation in FLI against the *M*-PDFF ($R^2 = 0.347$) is shown in Fig 2(b).

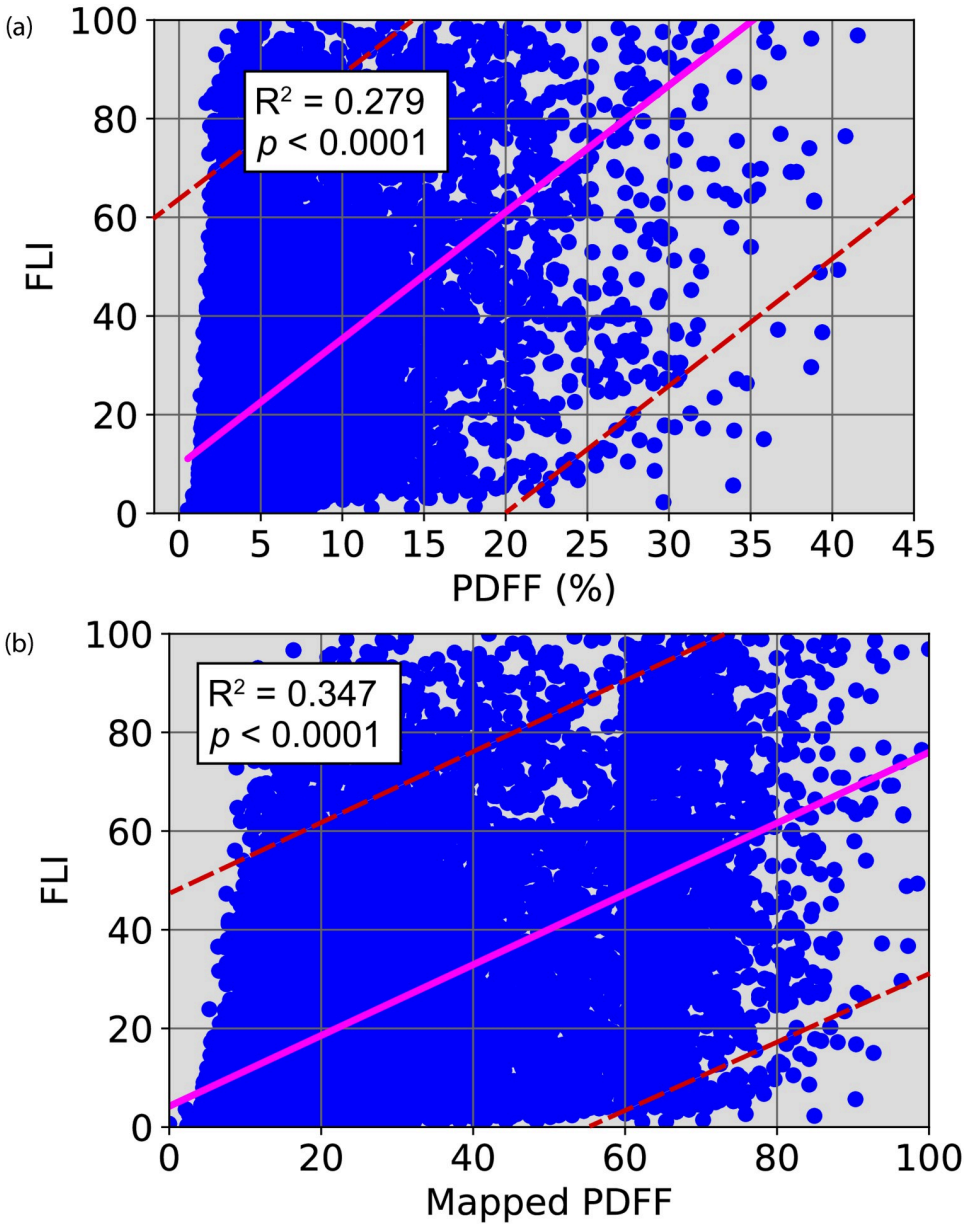

Fig 2. (a) Correlation of fatty liver index (FLI) against respective proton density fat fraction (PDFF); (b) Relationship between FLI and the mapped PDFF. (a) FLI versus PDFF. (b) FLI versus mapped PDFF.

https://doi.org/10.1371/journal.pone.0273171.g002

Feature importance

Input variable importances for the models are shown in Fig 3. The FLI had a significant impact on each model's output. Model 1 integrated all 18 variables while Model 2 excluded T2D status, HbA1c and HDL cholesterol to mitigate opposite serum levels in subjects with NAFLD and ALD. Model 3 further excluded serum biochemistry variables that did not significantly impact the resultant R^2 statistic, MAE or SD, including white blood cell (WBC) count, glucose and triglycerides as an independent variable albeit integrated into the computation of FLI. Thus, Model 3 was selected as the resultant regression model to predict FLI+ by integrating 12

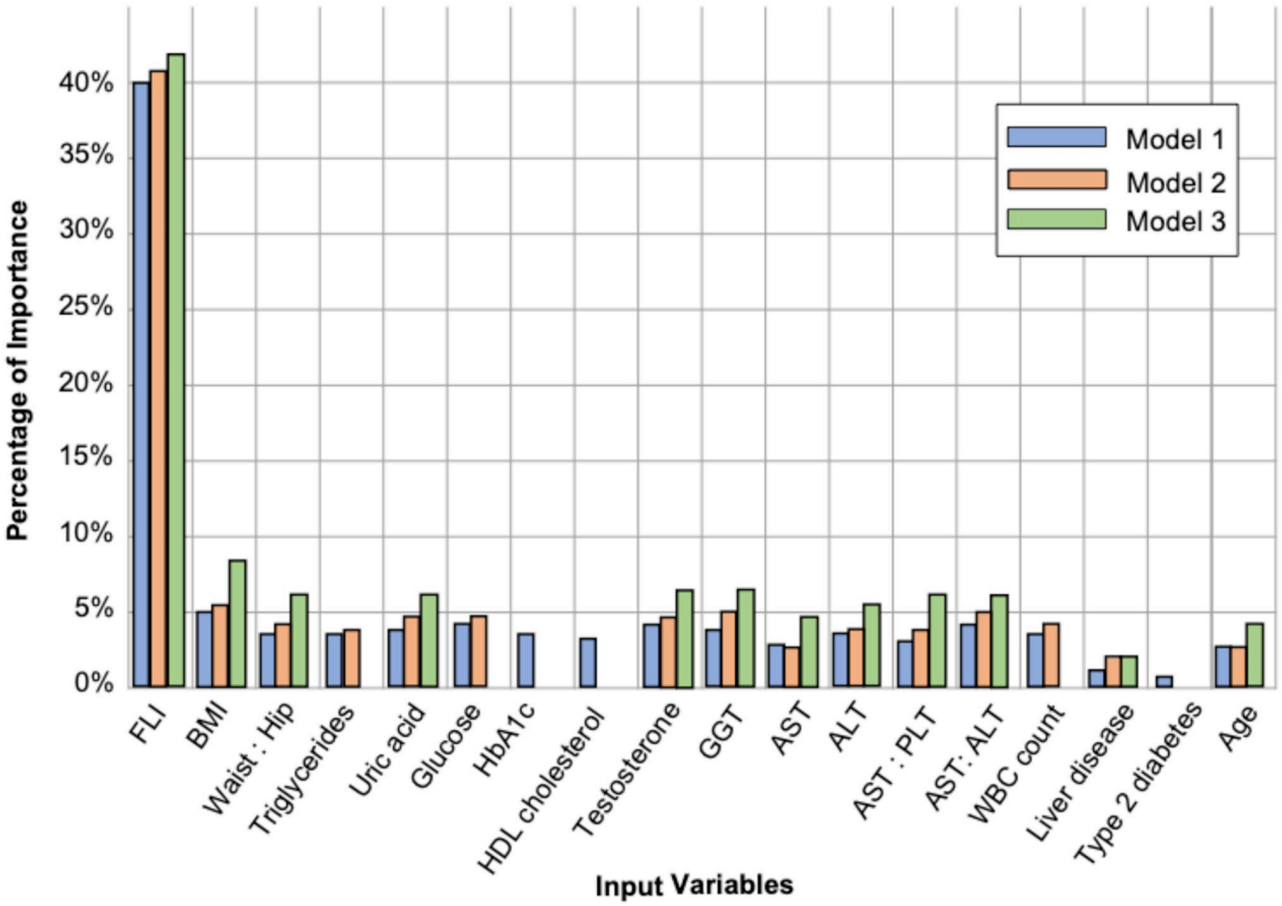

Fig 3. Input variable importance in the three models.

https://doi.org/10.1371/journal.pone.0273171.g003

input variables including FLI (41%), BMI (7.5%), the waist-to-hip ratio (5.9%), uric acid (6.0%), testosterone (6.4%), GGT (6.3%), AST (4.5%), ALT (5.6%), AST to ALT ratio (5.7%), AST to platelet count ratio (5.7%), liver disease diagnosis (1.0%) and age (4.4%).

Performance of FLI+

The MAE, SD and adjusted R^2 statistic for FLI+ and corresponding FLI were evaluated against the target *M*-PDFF across a four-fold CV to assess the robustness in the proposed gradient boosting model's performance (Table 3). There was a slight variation for each fold (SD 0.01 to 0.16) for FLI+, as shown in the second to the fourth columns. The FLI+ outperformed the original FLI by delivering a lower MAE by approximately 47%, a lower SD by approximately 20% and an increased adjusted R^2 statistic by approximately 49%, reflecting a more accurate representation of liver fat content.

The 95% prediction intervals between FLI+ and *M*-PDFF for all test subjects for one CV fold ($R^2 = 0.557$) is shown in Fig 4(a), while Fig 4(b) provides insight between the corresponding FLI and *M*-PDFF in the same CV fold ($R^2 = 0.372$). Notice that for a *M*-PDFF of 40, the resultant FLI values overflowed the entire 0–100 range, whereas FLI+ resulted in a tighter predicted range of 10–70. Moreover, FLI+ outperformed FLI between a *M*-PDFF of 40–100 in the upper prediction interval region. Moreover, FLI+ achieved an improved score in both the

Table 3. Performance of FLI+ versus FLI.

CV-Fold	FLI+			FLI		
	MAE	SD	R^2	MAE	SD	R^2
1	7.67	10.5	0.557	14.3	13.2	0.372
2	7.87	10.7	0.535	14.8	12.9	0.369
3	7.61	10.4	0.552	14.4	13.2	0.371
4	7.83	10.8	0.520	14.7	13.8	0.334
Mean	7.75	10.6	0.541	14.6	13.3	0.362

Four-fold cross-validation (CV) results of mean absolute error (MAE), standard deviation (SD) and coefficient of determination (R^2) of fatty liver index (FLI)+ and FLI when compared to mapped proton density fat fraction (PDFF) interpolated to FLI range and threshold.

https://doi.org/10.1371/journal.pone.0273171.t003

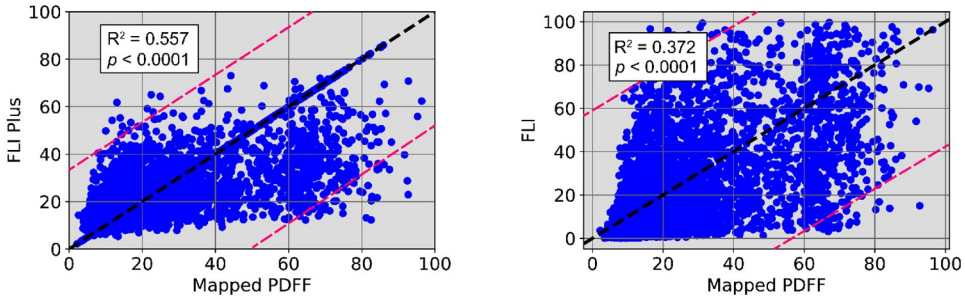

Fig 4. Correlation of fatty liver index (FLI) Plus (a) FLI (b) with proton density fat fraction (PDFF) mapped to the FLI risk range and threshold. (a) FLI+ versus mapped PDFF. (b) FLI versus mapped PDFF.

https://doi.org/10.1371/journal.pone.0273171.g004

upper and lower prediction intervals for a *M*-PDFF between 0–40 compared to FLI. For example, for a *M*-PDFF of 20, FLI spanned 0–98, whereas FLI+ delivered a more accurate and conservative range of 10–65. Another method of comparison using Bland-Altman plots is provided in Fig A in S1 File.

To assess the performance of FLI+ in every risk group, we compared the average MAE and SD (Table 4) and found a higher MAE in the elevated and severe groups by approximately two to five times compared to the normal group, with comparable SD across all three groups. There was a higher degree of accuracy in the upper interval for the severe group between approximately 40 and 80 *M*-PDFF as shown in Fig 4(a).

FLI+ achieved an improvement in MAE that was approximately two times lower compared to FLI in the elevated and normal groups with 10.6 versus 20.9 and 4.80 versus 11.0, respectively. FLI+ also achieved an improved MAE in the severe group that is lower by approximately 0.8 compared to FLI, suggesting the relatively higher variation in PDFF shown

Table 4. Mean performance of FLI+ and FLI stratified by risk groups.

Risk	MAE		SD	
	FLI+	FLI	FLI+	FLI
Normal	4.80	11.0	5.92	10.6
Elevated	10.6	20.9	10.5	13.4
Severe	21.5	25.8	17.9	16.8

https://doi.org/10.1371/journal.pone.0273171.t004

Table 5. Percentage of predicted FLI+ values with lower absolute error compared to original computed FLI.

Risk	Mapped PDFF to FLI	FLI+
Normal	$0 \leq$ M-PDFF < 30	77.7%
Elevated	$30 \leq$ M-PDFF < 60	78.0%
Severe	$60 \leq$ M-PDFF ≤ 100	58.1%

https://doi.org/10.1371/journal.pone.0273171.t005

in Fig 1(b) might have impacted the robustness of the prediction model. Table 5 shows for each risk group the average percentage of FLI+ having a score with a lower absolute error than its corresponding FLI. The severe group achieved a more accurate prediction in 58.1% of subjects, whereas the normal and elevated groups achieved a more accurate prediction in more than 77.0% of subjects.

Receiver operator characteristic (ROC) curves were constructed for each of the three groups (normal, elevated and severe) as shown in Fig 5(a). The average area under the ROC curve (AUROC) resulted in 0.86 (95%CI 0.79,0.91) and highlights the ability of FLI+ to discriminate between subjects with and without fatty liver. By comparison, Fig 5(b) illustrates that FLI resulted in an AUROC of 0.79 (95%CI 0.72,0.84).

The diagnostic accuracy of FLI+ to predict fatty liver by five-unit intervals, as per the original study [24], is provided in Table 6(a) and reports the percentage of subjects (%), SN, SP, LR + and LR−. For example, a cut-off point of FLI+ $\geq$ 10 resulted in an LR− of 0.25, indicating a four-fold decrease in the odds of having fatty liver given a negative test result. Moreover, the same cut-off point was moderate at ruling in fatty liver given a positive test result with an LR + of 6.94.

The corresponding predictive scores of FLI scores are shown in Table 6(b), where an FLI + and FLI cut-point $\geq$10 had a sensitivity of 0.78 versus 0.58, respectively. An FLI+ cut-point $\geq$ 60 resulted in a specificity of 0.97 versus 0.72 in FLI and a significantly different LR + of 27.6 versus 1.53, respectively. In other words, given a cut-off point of FLI+ $\geq$ 60, an LR + of 27.6 indicates a 28-fold increase in the odds of ruling in fatty liver given a positive test result. An LR− of 0.07 delivered a 14-fold decrease in the odds of having excess liver fat given a negative test result.

Application of FLI+ to an additional UK Biobank dataset

To further compare the outcome between FLI+ and FLI, we applied our methods to the wider UK Biobank cohort who were not part of the imaging sub-study (N = 373, 255). Since these

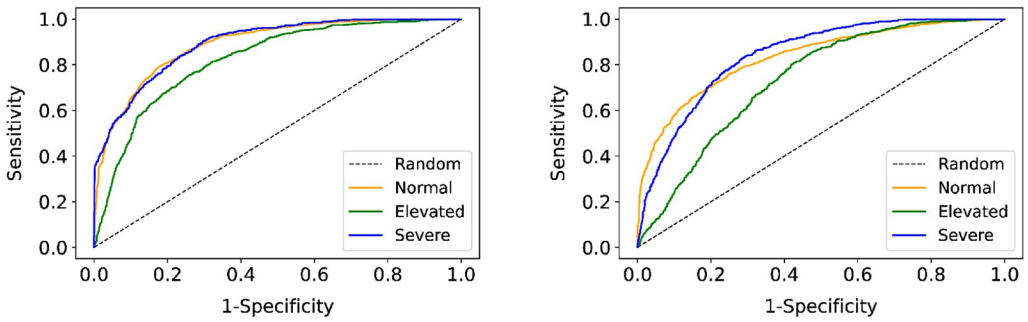

Fig 5. Receiver operating characteristic (ROC) curves for (a) FLI+ and (b) FLI to distinguish the presence or absence of fatty liver. Normal group represents non-fatty liver whereas elevated and severe represent fatty liver. (a) FLI+. (b) FLI.

https://doi.org/10.1371/journal.pone.0273171.g005

Table 6. FLI+ and FLI cut-point table.

CP	%	SN	SP	LR+	LR−
≥10	91.2	0.78	0.89	6.94	0.25
≥20	45.9	0.65	0.82	3.68	0.43
≥30	24.4	0.55	0.77	2.41	0.59
≥40	13.0	0.64	0.82	3.62	0.43
≥50	7.19	0.79	0.89	7.33	0.24
≥60	4.22	0.93	0.97	27.6	0.07

(a) FLI+

CP	%	SN	SP	LR+	LR−
≥10	57.2	0.58	0.79	2.79	0.53
≥20	39.3	0.50	0.75	2.00	0.67
≥30	28.7	0.44	0.72	1.60	0.77
≥40	20.8	0.42	0.71	1.44	0.82
≥50	15.0	0.40	0.70	1.34	0.86
≥60	9.97	0.43	0.72	1.53	0.79

(b) FLI

Fatty liver index (FLI)+ (a) and FLI (b) cut-point table by five-unit intervals. Abbreviations: CP = cut-point; % = proportion of patients with an FLI+ and FLI cut-point; SN = sensitivity; SP = specificity; LR+ = positive likelihood ratio; LR− = negative likelihood ratio.

https://doi.org/10.1371/journal.pone.0273171.t006

participants had not undergone imaging, no liver PDFF measurements were available. This cohort was aged 37–73 years, with an approximately equal proportion of male and female subjects, of whom 32% were in the healthy BMI range, 43% were overweight and 25% were obese. The FLI algorithm resulted in a median score of 16.7 (IQR 5.5–41.5), whereas the model predicting FLI+ delivered a median of 21.4 (IQR 14.3–32.5). A summary of the anthropometric, biochemical and clinical subject characteristics are provided in Table C in S1 File and additional supporting information is provided in Text C in S1 File, Tables D–F in S1 File.

Discussion

This paper presents a predictive regression model using a gradient boosting algorithm to calculate FLI+ as a score between 0 and 100, reflecting a subject's liver fat level. The proposed model was rigorously evaluated using four-fold cross validation, in which the predicted FLI + outperformed the original FLI with an increased R^2 statistic and significantly lower mean absolute error and standard deviation, demonstrating consistency in performance with potential for clinical translation.

The proposed predictive model utilised a UK Biobank dataset containing 28,796 estimates of MRI-derived PDFF across normal to severe levels, and integrated the following input variables: age, the waist-to-hip ratio, BMI, original computed FLI, uric acid, testosterone, GGT, AST, ALT, the ratio of AST to ALT, the ratio of AST to PLT and liver disease diagnosis.

We have shown that approximately 4% of all subjects evaluated in the context of this study had an FLI+ $\geq$ 60, whereas approximately twice as many had the same FLI cut-point. Similarly, approximately 10% of subjects had an FLI+ $<$ 10, whereas approximately 40% had the same FLI cut-point. In this study, a subject without fatty liver was approximately four times more likely to have an FLI+ $<$ 10, and a subject with fatty liver was approximately 28 times more likely to have an FLI+ $\geq$ 60. In contrast, a subject without fatty liver was approximately two times more likely to have an FLI $<$ 10 and a subject with fatty liver was approximately 1.5

times more likely to have an FLI $\geq$ 60. Considering the original study that derived the FLI algorithm using abdominal ultrasound [24], the ground-truth used in the development of a regression model predicting FLI+ was MRI-derived PDFF estimates of liver fat content. We note that the original study had a sensitivity of 0.55 for predicting in favour of fatty liver at a FLI $\geq$ 30, while FLI+ had a lower sensitivity by approximately 1.5 times. However, if the cut-off point of the FLI was $\geq$60 to rule in favour of fatty liver at a sensitivity of 0.61, as in the original study, the sensitivity for FLI+ increased to 0.93.

By evaluating our predictive model, the FLI+ score discriminates between subjects with normal and elevated or severe fatty liver ($\geq$5%) and achieves an AUROC of 0.86. We have also shown that the FLI+ score compared to FLI is 77.7% more accurate in predicting normal liver and 78.0% and 58.1% more accurate in predicting elevated and severe fatty liver, respectively.

The FLI has been previously examined against gold-standard measurements of quantitative liver fat derived from MRI in the last decade. However, these studies involved relatively small cohorts, often characterised by a specific gender or health status. For example, Bozkurt et al. [71] reported a study involving 26 female subjects, 17 diagnosed with previous gestational diabetes (pGDM) and eight with normal glucose tolerance during pregnancy, all of whom underwent ^{1}H-MRS and demonstrated a strong nonlinear relationship between FLI and liver fat content with limited predictive ability. Another study involving ^{1}H-MRS and 92 non-diabetic, predominantly non-obese subjects achieved AUROC = 0.72 for the FLI and related positively to fatty liver [72]. Using ^{1}H-MRS to measure liver fat as the gold-standard, the discriminative ability of FLI was demonstrated in Cuthbertson et al. [44] involving 168 subjects with NAFLD and 168 healthy controls with AUROC = 0.79; however, the FLI could not quantitatively predict liver fat. Interestingly, the inclusion of a dual-echo chemical shift imaging MRI technique in a more extensive study involving 392 and 909 subjects with and without NAFLD subjects, respectively, reported a lower diagnostic performance of AUROC = 0.68 for FLI [73].

As a non-invasive method, predicting FLI+ can improve stratification between absent, mild, moderate and severe fatty liver in a large cohort of subjects without the expensive costs of frequent MR imaging. Thus, researchers that aim to investigate changes in accumulated liver fat due to interventions in diet or exercise can integrate the FLI+ score as a valuable marker to screen for the presence of or severity of fatty liver throughout a clinical study.

It is worth pointing out that the blood chemistry tests in the UK Biobank were performed at the initial assessment visit, and the MRI was performed during subsequent visits. Furthermore, whereas the original study introducing the FLI algorithm integrated blood markers measured after eight hours of fasting, a limitation of this study is that only non-fasted blood samples were available in the UK Biobank. Thus, although we analysed glucose levels in the context of this study, we also analysed the HbA1c marker, which does not require fasting. Previous research has shown that results obtained from non-fasting versus fasting glucose in large-scale studies are not statistically significant. Moreover, a recently published study involving 8,270 subjects showed excellent 94.8% agreement between fasting and non-fasting cholesterol levels [74]. We recognise that non-fasting triglycerides, GGT and testosterone measures [75, 76] could impact the predictive modelling outcome depending on the period lapsed between a participant's blood test and their last intake of high carbohydrates.

Indeed, we also acknowledge that the FLI+ indicates the level of accumulated fat in the liver without discriminating between ALD, NAFLD or metabolic dysfunction in NAFLD. Moreover, we recognise that the level of liver fat does not always correspond to disease severity. For example, individuals with NASH-related cirrhosis have a reduced quantitative liver fat content than those with early-stage NAFLD. Consequently, the FLI+ score can integrate into a medical study or assessment alongside the individual's dietary factors and possible external symptoms that might support characterising their condition.

An additional limitation of this study is the large imbalance of genetic ancestry groups in which over 98% of subjects were white European. Future work might seek to obtain and integrate data from a variety of subject demographics, including African, Central and South Asian and East Asian ancestry. We also acknowledge that this study has an imbalance in the proportion of subjects having fatty liver compared to non-fatty. Future work could explore techniques to counter the data imbalance when developing a model to predict a more accurate FLI reflective of a subject's level of liver fat. However, this study had the advantage of utilising an MRI-PDFF dataset of 28,796 subjects with normal liver fat and varying levels of fatty liver that reflects the general population. While this study using FLI achieved AUROC comparable to previous works, FLI+ consistently improved the discriminative ability across all risk levels.

Future research will compare the FLI+ with available indices that have been previously derived to identify subjects with a form of fatty liver as inferred using ^{1}H-MRS or ultrasound, including the NAFLD liver fat score [77], Hepatic steatosis index (HSI) [78], ZJU index [79], Framingham steatosis index (FSI) [80] and the Dallas steatosis index (DSI) [81]. Although these indices were derived initially using fasting blood markers, a recent study performed an external validation on the DSI in the UK Biobank cohort [82] and reported that while the DSI does not discriminate between subjects with NAFLD and those with NASH, it is a valid algorithm to predict NAFLD. The FSI and DSI also integrate information about a subject's diagnosis of hypertension and diabetes, and the NAFLD liver fat score requires diagnosis relating to metabolic syndrome, unlike the FLI+ score that is primarily based on anthropometry, blood markers and liver disease diagnosis.

Subsequent work will also investigate deep learning regression techniques to increase the prediction accuracy closer to the quantitative level of liver fat. Depending on the nature of a clinician's workflow, it may be preferable to utilise a model that predicts a subject's category of liver fat. Thus, future work may build upon the regression model to introduce a classification model that predicts a single category of normal, elevated or severe fatty liver.

Conclusions

By integrating the most extensive MRI dataset from the UK Biobank, we developed a regression model that predicts FLI+ as an improvement to FLI in a large cohort reflective of the general adult population. Obtaining an FLI+ score requires four basic anthropometric measurements and a standard set of seven biochemical blood variables readily obtainable in clinical and research settings.

The FLI+ has the potential to improve diagnosis and provide a more accurate stratification than FLI between absent, mild, moderate and severe levels of hepatic steatosis. In addition, the model predicting FLI+ can be easily used as a standalone tool or integrated into a more extensive computational system for research or clinical purposes.

Supporting information

S1 File. This file contains the supplementary information: Texts A–C, Tables A–F, and Figs A–C.
(PDF)

Acknowledgments

This study was carried out using UK Biobank Application number 23889, and we thank all the participants in the UK Biobank study. The authors received no specific funding for this work.

Author Contributions

Conceptualization: Hykoush A. Asaturyan, Brandon Whitcher, E. Louise Thomas, Jimmy D. Bell.

Data curation: Hykoush A. Asaturyan, Nicolas Basty, Marjola Thanaj, Brandon Whitcher.

Formal analysis: Hykoush A. Asaturyan.

Funding acquisition: E. Louise Thomas.

Investigation: Jimmy D. Bell.

Methodology: Hykoush A. Asaturyan, Nicolas Basty, Brandon Whitcher.

Project administration: Brandon Whitcher.

Software: Hykoush A. Asaturyan.

Supervision: Brandon Whitcher, E. Louise Thomas, Jimmy D. Bell.

Validation: Hykoush A. Asaturyan.

Visualization: Hykoush A. Asaturyan.

Writing – original draft: Hykoush A. Asaturyan, Nicolas Basty, Marjola Thanaj, Brandon Whitcher, E. Louise Thomas, Jimmy D. Bell.

Writing – review & editing: Hykoush A. Asaturyan, Nicolas Basty, Marjola Thanaj, Brandon Whitcher, E. Louise Thomas, Jimmy D. Bell.

References

1. European Association for the Study of The Liver and European Association for the Study of Diabetes (EASD) and others. EASL-EASD-EASO Clinical Practice Guidelines for the management of non-alcoholic fatty liver disease. Obesity Facts. 2016; 9(2):65–90. https://doi.org/10.1159/000443344
2. Petagine L, Zariwala MG, Patel VB. Alcoholic liver disease: Current insights into cellular mechanisms. World Journal of Biological Chemistry. 2021; 12(5):87. https://doi.org/10.4331/wjbc.v12.i5.87 PMID: 34630912
3. Pandyarajan V, Gish RG, Alkhouri N, Noureddin M. Screening for nonalcoholic fatty liver disease in the primary care clinic. Gastroenterology & Hepatology. 2019; 15(7):357. PMID: 31391806
4. Zhang P, Wang W, Mao M, Gao R, Shi W, Li D, et al. Similarities and Differences: A Comparative Review of the Molecular Mechanisms and Effectors of NAFLD and AFLD. Frontiers in Physiology. 2021; p. 1130. https://doi.org/10.3389/fphys.2021.710285 PMID: 34393826
5. Mantovani A, Scorletti E, Mosca A, Alisi A, Byrne CD, Targher G. Complications, morbidity and mortality of nonalcoholic fatty liver disease. Metabolism. 2020; 111:154170. https://doi.org/10.1016/j.metabol.2020.154170 PMID: 32006558
6. Rinaldi L, Pafundi PC, Galiero R, Caturano A, Morone MV, Silvestri C, et al. Mechanisms of non-alcoholic fatty liver disease in the metabolic syndrome. A narrative review. Antioxidants. 2021; 10(2):270. https://doi.org/10.3390/antiox10020270 PMID: 33578702
7. Acierno C, Caturano A, Pafundi P, Nevola R, Adinolfi L, Sasso F. Nonalcoholic fatty liver disease and type 2 diabetes: Pathophysiological mechanisms shared between the two faces of the same coin. Explor Med. 2020; 1:287–306.
8. Caturano A, Acierno C, Nevola R, Pafundi PC, Galiero R, Rinaldi L, et al. Non-alcoholic fatty liver disease: From pathogenesis to clinical impact. Processes. 2021; 9(1):135. https://doi.org/10.3390/pr9010135
9. Younossi ZM, Koenig AB, Abdelatif D, Fazel Y, Henry L, Wymer M. Global epidemiology of nonalcoholic fatty liver disease—meta-analytic assessment of prevalence, incidence, and outcomes. Hepatology. 2016; 64(1):73–84. https://doi.org/10.1002/hep.28431 PMID: 26707365
10. Rinella ME. Nonalcoholic fatty liver disease: a systematic review. JAMA. 2015; 313(22):2263–2273. https://doi.org/10.1001/jama.2015.5370 PMID: 26057287

11. Anderson EL, Howe LD, Jones HE, Higgins JP, Lawlor DA, Fraser A. The prevalence of non-alcoholic fatty liver disease in children and adolescents: a systematic review and meta-analysis. PloS ONE. 2015; 10(10):e0140908. https://doi.org/10.1371/journal.pone.0140908 PMID: 26512983

12. Younossi Z, Tacke F, Arrese M, Chander Sharma B, Mostafa I, Bugianesi E, et al. Global perspectives on nonalcoholic fatty liver disease and nonalcoholic steatohepatitis. Hepatology. 2019; 69(6):2672–2682. https://doi.org/10.1002/hep.30251 PMID: 30179269

13. Younossi ZM. Non-alcoholic fatty liver disease–A global public health perspective. Journal of Hepatology. 2019; 70(3):531–544. https://doi.org/10.1016/j.jhep.2018.10.033 PMID: 30414863

14. Kaya E, Yilmaz Y. Non-alcoholic Fatty Liver Disease: A Global Public Health Issue. In: Obesity and Diabetes. Springer; 2020. p. 321–333.

15. Anstee QM, Day CP. The genetics of NAFLD. Nature Reviews Gastroenterology & Hepatology. 2013; 10(11):645–655. https://doi.org/10.1038/nrgastro.2013.182

16. Mantovani A, Byrne CD, Bonora E, Targher G. Nonalcoholic fatty liver disease and risk of incident type 2 diabetes: a meta-analysis. Diabetes Care. 2018; 41(2):372–382. https://doi.org/10.2337/dc17-1902 PMID: 29358469

17. Assy N, Kaita K, Mymin D, Levy C, Rosser B, Minuk G. Fatty infiltration of liver in hyperlipidemic patients. Digestive Diseases and Sciences. 2000; 45(10):1929–1934. https://doi.org/10.1023/A:1005661516165 PMID: 11117562

18. Zhao YC, Zhao GJ, Chen Z, She ZG, Cai J, Li H. Nonalcoholic fatty liver disease: an emerging driver of hypertension. Hypertension. 2020; 75(2):275–284. https://doi.org/10.1161/HYPERTENSIONAHA.119.13419 PMID: 31865799

19. Kasper P, Martin A, Lang S, Kütting F, Goeser T, Demir M, et al. NAFLD and cardiovascular diseases: a clinical review. Clinical Research in Cardiology. 2021; 110(7):921–937. https://doi.org/10.1007/s00392-020-01709-7 PMID: 32696080

20. Tana C, Ballestri S, Ricci F, Di Vincenzo A, Ticinesi A, Gallina S, et al. Cardiovascular risk in non-alcoholic fatty liver disease: mechanisms and therapeutic implications. International Journal of Environmental Research and Public Health. 2019; 16(17):3104. https://doi.org/10.3390/ijerph16173104 PMID: 31455011

21. Byrne CD, Targher G. NAFLD as a driver of chronic kidney disease. Journal of Hepatology. 2020; 72(4):785–801. https://doi.org/10.1016/j.jhep.2020.01.013 PMID: 32059982

22. Zhang M, Lin S, Wang Mf, Huang Jf, Liu Sy, Wu Sm, et al. Association between NAFLD and risk of prevalent chronic kidney disease: why there is a difference between east and west? BMC Gastroenterology. 2020; 20(1):1–7. https://doi.org/10.1186/s12876-020-01278-z PMID: 32375660

23. Lombardi R, Petta S, Pisano G, Dongiovanni P, Rinaldi L, Adinolfi LE, et al. FibroScan identifies patients with nonalcoholic fatty liver disease and cardiovascular damage. Clinical Gastroenterology and Hepatology. 2020; 18(2):517–519. https://doi.org/10.1016/j.cgh.2018.11.011 PMID: 30528844

24. Bedogni G, Bellentani S, Miglioli L, Masutti F, Passalacqua M, Castiglione A, et al. The Fatty Liver Index: a simple and accurate predictor of hepatic steatosis in the general population. BMC Gastroenterology. 2006; 6(1):1–7. https://doi.org/10.1186/1471-230X-6-33 PMID: 17081293

25. Idilman IS, Aniktar H, Idilman R, Kabacam G, Savas B, Elhan A, et al. Hepatic steatosis: quantification by proton density fat fraction with MR imaging versus liver biopsy. Radiology. 2013; 267(3):767–775. https://doi.org/10.1148/radiol.13121360 PMID: 23382293

26. Cunha GM, Thai TT, Hamilton G, Covarrubias Y, Schlein A, Middleton MS, et al. Accuracy of common proton density fat fraction thresholds for magnitude-and complex-based chemical shift-encoded MRI for assessing hepatic steatosis in patients with obesity. Abdominal Radiology. 2020; 45(3):661–671. https://doi.org/10.1007/s00261-019-02350-3 PMID: 31781899

27. Caussy C, Brissot J, Singh S, Bassirian S, Hernandez C, Bettencourt R, et al. Prospective, Same-Day, Direct Comparison of Controlled Attenuation Parameter With the M vs the XL Probe in Patients With Nonalcoholic Fatty Liver Disease, Using Magnetic Resonance Imaging–Proton Density Fat Fraction as the Standard. Clinical Gastroenterology and Hepatology. 2020; 18(8):1842–1850. https://doi.org/10.1016/j.cgh.2019.11.060 PMID: 31843596

28. Shin J, Kim MJ, Shin HJ, Yoon H, Kim S, Koh H, et al. Quick assessment with controlled attenuation parameter for hepatic steatosis in children based on MRI-PDFF as the gold standard. BMC Pediatrics. 2019; 19(1):1–9. https://doi.org/10.1186/s12887-019-1485-8 PMID: 30987634

29. Wang JH, Ou HY, Yen YH, Chen CH, Lu SN. Usefulness of controlled attenuation parameter in detecting and monitoring hepatic steatosis with MRI-PDFF as reference. Digestive Diseases and Sciences. 2020; 65(5):1512–1519. https://doi.org/10.1007/s10620-019-05883-1 PMID: 31617130

30. Caussy C, Alquiraish MH, Nguyen P, Hernandez C, Cepin S, Fortney LE, et al. Optimal threshold of controlled attenuation parameter with MRI-PDFF as the gold standard for the detection of hepatic steatosis. Hepatology. 2018; 67(4):1348–1359. https://doi.org/10.1002/hep.29639 PMID: 29108123

31. Wilman HR, Kelly M, Garratt S, Matthews PM, Milanesi M, Herlihy A, et al. Characterisation of liver fat in the UK Biobank cohort. PloS ONE. 2017; 12(2):e0172921. https://doi.org/10.1371/journal.pone.0172921 PMID: 28241076

32. Caussy C, Reeder SB, Sirlin CB, Loomba R. Noninvasive, quantitative assessment of liver fat by MRI-PDFF as an endpoint in NASH trials. Hepatology. 2018; 68(2):763–772. https://doi.org/10.1002/hep.29797 PMID: 29356032

33. Dennis A, Kelly MD, Fernandes C, Mouchti S, Fallowfield JA, Hirschfield G, et al. Correlations between MRI biomarkers PDFF and cT1 with histopathological features of non-alcoholic steatohepatitis. Frontiers in Endocrinology. 2021; 11:1053. https://doi.org/10.3389/fendo.2020.575843 PMID: 33584535

34. Huang X, Xu M, Chen Y, Peng K, Huang Y, Wang P, et al. Validation of the fatty liver index for nonalcoholic fatty liver disease in middle-aged and elderly Chinese. Medicine. 2015; 94(40). https://doi.org/10.1097/MD.0000000000001682 PMID: 26448014

35. Drinda S, Grundler F, Neumann T, Lehmann T, Steckhan N, Michalsen A, et al. Effects of periodic fasting on fatty liver index—a prospective observational study. Nutrients. 2019; 11(11):2601. https://doi.org/10.3390/nu11112601 PMID: 31671589

36. Chen LW, Huang PR, Chien CH, Lin CL, Chien RN. A community-based study on the application of fatty liver index in screening subjects with nonalcoholic fatty liver disease. Journal of the Formosan Medical Association. 2020; 119(1):173–181. https://doi.org/10.1016/j.jfma.2019.03.016 PMID: 30981560

37. Cuthbertson DJ, Koskinen J, Brown E, Magnussen CG, Hutri-Kähönen N, Sabin M, et al. Fatty liver index predicts incident risk of prediabetes, type 2 diabetes and non-alcoholic fatty liver disease (NAFLD). Annals of Medicine. 2021; 53(1):1257–1265. https://doi.org/10.1080/07853890.2021.1956685

38. Castellana M, Donghia R, Guerra V, Procino F, Lampignano L, Castellana F, et al. Performance of Fatty Liver Index in Identifying Non-Alcoholic Fatty Liver Disease in Population Studies. A Meta-Analysis. Journal of Clinical Medicine. 2021; 10(9):1877. https://doi.org/10.3390/jcm10091877 PMID: 33925992

39. Franch-Nadal J, Caballeria L, Mata-Cases M, Mauricio D, Giraldez-García C, Mancera J, et al. Fatty liver index is a predictor of incident diabetes in patients with prediabetes: The PREDAPS study. PloS ONE. 2018; 13(6):e0198327. https://doi.org/10.1371/journal.pone.0198327 PMID: 29856820

40. Khang AR, Lee HW, Yi D, Kang YH, Son SM. The fatty liver index, a simple and useful predictor of metabolic syndrome: analysis of the Korea National Health and Nutrition Examination Survey 2010–2011. Diabetes, Metabolic Syndrome and Obesity: Targets and Therapy. 2019; 12:181. https://doi.org/10.2147/DMSO.S189544 PMID: 30774403

41. Zou B, Yeo YH, Cheung R, Ingelsson E, Nguyen MH. Fatty Liver Index and Development of Cardiovascular Disease: Findings from the UK Biobank. Digestive Diseases and Sciences. 2021; 66(6):2092–2100. https://doi.org/10.1007/s10620-021-06954-y PMID: 33782808

42. Olubamwo OO, Virtanen JK, Pihlajamaki J, Mantyselka P, Tuomainen TP. Fatty liver index as a predictor of increased risk of cardiometabolic disease: finding from the Kuopio Ischaemic Heart Disease Risk Factor Study Cohort. BMJ Open. 2019; 9(9):e031420. https://doi.org/10.1136/bmjopen-2019-031420 PMID: 31492793

43. Zelber-Sagi S, Webb M, Assy N, Blendis L, Yeshua H, Leshno M, et al. Comparison of fatty liver index with noninvasive methods for steatosis detection and quantification. World Journal of Gastroenterology: WJG. 2013; 19(1):57. https://doi.org/10.3748/wjg.v19.i1.57 PMID: 23326163

44. Cuthbertson DJ, Weickert MO, Lythgoe D, Sprung VS, Dobson R, Umpleby A, et al. External validation of the fatty liver index and lipid accumulation product indices, using 1H-magnetic resonance spectroscopy, to identify hepatic steatosis in healthy controls and obese, insulin-resistant individuals. European Journal of Endocrinology. 2014; 171(5):561–569. https://doi.org/10.1530/EJE-14-0112 PMID: 25298375

45. Chen CH, Chen YY, Chuang CL, Chiang LM, Chiao SM, Hsieh KC. The study of anthropometric estimates in the visceral fat of healthy individuals. Nutrition Journal. 2014; 13(1):1–8. https://doi.org/10.1186/1475-2891-13-46

46. Lee KS, Kim HY, Lee SJ, Kwon SO, Na S, Hwang HS, et al. Prediction of newborn's body mass index using nationwide multicenter ultrasound data: a machine-learning study. BMC Pregnancy and Childbirth. 2021; 21(1):1–10. https://doi.org/10.1186/s12884-021-03660-5 PMID: 33653299

47. Hussain SA, Cavus N, Sekeroglu B. Hybrid Machine Learning Model for Body Fat Percentage Prediction Based on Support Vector Regression and Emotional Artificial Neural Networks. Applied Sciences. 2021; 11(21):9797. https://doi.org/10.3390/app11219797

48. Merrill Z, Chambers A, Cham R. Development and validation of body fat prediction models in American adults. Obesity Science & Practice. 2020; 6(2):189–195. https://doi.org/10.1002/osp4.392 PMID: 32313677

49. Shao YE. Body fat percentage prediction using intelligent hybrid approaches. The Scientific World Journal. 2014; 2014. https://doi.org/10.1155/2014/383910 PMID: 24723804

50. Agrawal S, Klarqvist MD, Diamant N, Ellinor PT, Mehta NN, Philippakis A, et al. Association of machine learning-derived measures of body fat distribution in <40, 000 individuals with cardiometabolic diseases. medRxiv. 2021;.

51. Alberti KGM, Zimmet P, Shaw J. The metabolic syndrome—a new worldwide definition. The Lancet. 2005; 366(9491):1059–1062. https://doi.org/10.1016/S0140-6736(05)67402-8 PMID: 16182882

52. Littlejohns TJ, Holliday J, Gibson LM, Garratt S, Oesingmann N, Alfaro-Almagro F, et al. The UK Biobank imaging enhancement of 100,000 participants:rationale, data collection, management and future directions. Nature Communications. 2020; 11(1). https://doi.org/10.1038/s41467-020-15948-9 PMID: 32457287

53. Bydder M, Ghodrati V, Gao Y, Robson MD, Yang Y, Hu P. Constraints in Estimating the Proton Density Fat Fraction. Magnetic Resonance Imaging. 2020; 66:1–8. https://doi.org/10.1016/j.mri.2019.11.009 PMID: 31740195

54. Liu Y, Basty N, Whitcher B, Bell JD, Sorokin EP, van Bruggen N, et al. Genetic architecture of 11 organ traits derived from abdominal MRI using deep learning. eLife. 2021; 10. https://doi.org/10.7554/eLife.65554 PMID: 34128465

55. Chen C, Zhu Z, Mao Y, Xu Y, Du J, Tang X, et al. HbA1c may contribute to the development of non-alcoholic fatty liver disease even at normal-range levels. Bioscience Reports. 2020; 40(1):BSR20193996. https://doi.org/10.1042/BSR20193996 PMID: 31940026

56. Sattar N, Forrest E, Preiss D. Non-alcoholic fatty liver disease. BMJ. 2014; 349. https://doi.org/10.1136/bmj.g4596

57. Chung GE, Yim JY, Kim D, Kwak MS, Yang JI, Chung SJ, et al. Associations between white blood cell count and the development of incidental nonalcoholic fatty liver disease. Gastroenterology Research and Practice. 2016; 2016. https://doi.org/10.1155/2016/7653689 PMID: 28070183

58. Wang S, Zhang C, Zhang G, Yuan Z, Liu Y, Ding L, et al. Association between white blood cell count and non-alcoholic fatty liver disease in urban Han Chinese: a prospective cohort study. BMJ Open. 2016; 6(6):e010342. https://doi.org/10.1136/bmjopen-2015-010342 PMID: 27251683

59. Oral A, Sahin T, Turker F, Kocak E. Relationship between serum uric acid levels and nonalcoholic fatty liver disease in non-obese patients. Medicina. 2019; 55(9):600. https://doi.org/10.3390/medicina55090600 PMID: 31533345

60. Jensen T, Niwa K, Hisatome I, Kanbay M, Andres-Hernando A, Roncal-Jimenez CA, et al. Increased serum uric acid over five years is a risk factor for developing fatty liver. Scientific Reports. 2018; 8(1):1–8. https://doi.org/10.1038/s41598-018-30267-2 PMID: 30082907

61. Ren XY, Shi D, Ding J, Cheng ZY, Li HY, Li JS, et al. Total cholesterol to high-density lipoprotein cholesterol ratio is a significant predictor of nonalcoholic fatty liver: Jinchang cohort study. Lipids in Health and Disease. 2019; 18(1):1–7. https://doi.org/10.1186/s12944-019-0984-9 PMID: 30744645

62. Barbonetti A, Caterina Vassallo MR, Cotugno M, Felzani G, Francavilla S, Francavilla F. Low testosterone and non-alcoholic fatty liver disease: Evidence for their independent association in men with chronic spinal cord injury. The Journal of Spinal Cord Medicine. 2016; 39(4):443–449. https://doi.org/10.1179/2045772314Y.0000000288 PMID: 25614040

63. Sarkar M, Wellons M, Cedars MI, VanWagner L, Gunderson EP, Ajmera V, et al. Testosterone levels in pre-menopausal women are associated with nonalcoholic fatty liver disease in midlife. The American Journal of Gastroenterology. 2017; 112(5):755. https://doi.org/10.1038/ajg.2017.44 PMID: 28291240

64. Park JM, Lee HS, Oh J, Lee YJ. Serum testosterone level within normal range is positively associated with nonalcoholic fatty liver disease in premenopausal but not postmenopausal women. Journal of Women's Health. 2019; 28(8):1077–1082. https://doi.org/10.1089/jwh.2018.7263 PMID: 30653387

65. Bayard M, Holt JD, Boroughs E. Nonalcoholic fatty liver disease. American Family Physician. 2006; 73 (11):1961–1968. PMID: 16770927

66. Loaeza-del Castillo A, Paz-Pineda F, Oviedo-Cárdenas E, Sánchez-Avila F, Vargas-Vorácková F. AST to platelet ratio index (APRI) for the noninvasive evaluation of liver fibrosis. Annals of Hepatology. 2008; 7(4):350–357. https://doi.org/10.1016/S1665-2681(19)31836-8 PMID: 19034235

67. De Matteis C, Cariello M, Graziano G, Battaglia S, Suppressa P, Piazzolla G, et al. AST to Platelet Ratio Index (APRI) is an easy-to-use predictor score for cardiovascular risk in metabolic subjects. Scientific Reports. 2021; 11(1):1–14. https://doi.org/10.1038/s41598-021-94277-3 PMID: 34290320

68. Whitcher B, Thanaj M, Cule M, Liu Y, Basty N, Sorokin EP, et al. Precision MRI phenotyping enables detection of small changes in body composition for longitudinal cohorts. Scientific Reports. 2022; 12 (1):1–11. https://doi.org/10.1038/s41598-022-07556-y PMID: 35260612

69. Friedman JH. Stochastic gradient boosting. Computational Statistics & Data Analysis. 2002; 38(4):367–378. https://doi.org/10.1016/S0167-9473(01)00065-2

70. Shao Cx, Ye J, Dong Z, Li F, Lin Y, Liao B, et al. Steatosis grading consistency between controlled attenuation parameter and MRI-PDFF in monitoring metabolic associated fatty liver disease. Therapeutic Advances in Chronic Disease. 2021; 12:20406223211033119.

71. Bozkurt L, Göbl CS, Tura A, Chmelik M, Prikoszovich T, Kosi L, et al. Fatty liver index predicts further metabolic deteriorations in women with previous gestational diabetes. PloS ONE. 2012; 7(2):e32710. https://doi.org/10.1371/journal.pone.0032710 PMID: 22393439

72. Kahl S, Straßburger K, Nowotny B, Livingstone R, Klüppelholz B, Kessel K, et al. Comparison of liver fat indices for the diagnosis of hepatic steatosis and insulin resistance. PloS ONE. 2014; 9(4):e94059. https://doi.org/10.1371/journal.pone.0094059 PMID: 24732091

73. Jung TY, Kim MS, Hong HP, Kang KA, Jun DW. Comparative assessment and external validation of hepatic steatosis formulae in a community-based setting. Journal of Clinical Medicine. 2020; 9(9):2851. https://doi.org/10.3390/jcm9092851

74. Mora S, Chang CL, Moorthy MV, Sever PS. Association of nonfasting vs fasting lipid levels with risk of major coronary events in the Anglo-Scandinavian Cardiac Outcomes Trial–lipid lowering arm. JAMA Internal Medicine. 2019; 179(7):898–905. https://doi.org/10.1001/jamainternmed.2019.0392 PMID: 31135812

75. Lehtihet M, Arver S, Bartuseviciene I, Pousette Å. S-testosterone decrease after a mixed meal in healthy men independent of SHBG and gonadotrophin levels. Andrologia. 2012; 44(6):405–410. https://doi.org/10.1111/j.1439-0272.2012.01296.x PMID: 22524522

76. Caronia LM, Dwyer AA, Hayden D, Amati F, Pitteloud N, Hayes FJ. Abrupt decrease in serum testosterone levels after an oral glucose load in men: implications for screening for hypogonadism. Clinical Endocrinology. 2013; 78(2):291–296. https://doi.org/10.1111/j.1365-2265.2012.04486.x PMID: 22804876

77. Kotronen A, Peltonen M, Hakkarainen A, Sevastianova K, Bergholm R, Johansson LM, et al. Prediction of non-alcoholic fatty liver disease and liver fat using metabolic and genetic factors. Gastroenterology. 2009; 137(3):865–872. https://doi.org/10.1053/j.gastro.2009.06.005 PMID: 19524579

78. Lee JH, Kim D, Kim HJ, Lee CH, Yang JI, Kim W, et al. Hepatic steatosis index: a simple screening tool reflecting nonalcoholic fatty liver disease. Digestive and Liver Disease. 2010; 42(7):503–508. https://doi.org/10.1016/j.dld.2009.08.002 PMID: 19766548

79. Wang J, Xu C, Xun Y, Lu Z, Shi J, Yu C, et al. ZJU index: a novel model for predicting nonalcoholic fatty liver disease in a Chinese population. Scientific Reports. 2015; 5(1):1–10. https://doi.org/10.1038/srep16494 PMID: 26568423

80. Long MT, Pedley A, Colantonio LD, Massaro JM, Hoffmann U, Muntner P, et al. Development and validation of the Framingham steatosis index to identify persons with hepatic steatosis. Clinical Gastroenterology and Hepatology. 2016; 14(8):1172–1180. https://doi.org/10.1016/j.cgh.2016.03.034 PMID: 27046482

81. McHenry S, Park Y, Browning JD, Sayuk G, Davidson NO. Dallas steatosis index identifies patients with nonalcoholic fatty liver disease. Clinical Gastroenterology and Hepatology. 2020; 18(9):2073–2080. https://doi.org/10.1016/j.cgh.2020.01.020 PMID: 31982611

82. McHenry S, Park Y, Davidson NO. Validation of the Dallas steatosis index to predict nonalcoholic fatty liver disease in the UK Biobank population. Clinical Gastroenterology and Hepatology. 2021. https://doi.org/10.1016/j.cgh.2021.05.035 PMID: 34044131